Università di Pisa

Effects of quantum confinement and discrete dopants in nanoscale bulk Si MOSFETs

Gianluca Fiori
Dipartimento di Ingegneria dell'Informazione: Elettronica, Informatica, Telecomunicazioni, Università di Pisa
Giuseppe Iannaccone
Dipartimento di Ingegneria dell'Informazione: Elettronica, Informatica, Telecomunicazioni, Università di Pisa

G. Fiori, G. Iannaccone, *Effects of quantum confinement and discrete dopants in nanoscale bulk Si MOSFETs*, First IEEE Conference on Nanotechnology, p. 248, Maui, Hawaii, USA 2001 (IEEE, Piscataway).

Effects of quantum confinement and discrete dopants in nanoscale bulk-Si nMOSFET

G. Fiori, G. Iannaccone*
Dipartimento di Ingegneria dell'Informazione, Università degli studi di Pisa,
Via Diotisalvi 2, I-56122, Pisa, Italy
*g.iannaccone@iet.unipi.it

Abstract

We have developed a numerical code for the three-dimensional simulation of ultrashort channel MOSFETs considering the effects due to quantum confinement of electrons at the Si/SiO_2 interface. We have focused on the so-called "Well tempered" bulk-Si n-MOSFETs with channel length of 90, 50 and 25 nm proposed by D. Antoniadis. We found that the effect of quantum confinement on threshold voltage is of the order of 100 mV, and therefore justifies the effort for a quantum simulation of nanoscale MOSFETs. In addition, we have evaluated the effect of the random distribution of dopants, by simulating a large number of devices with uniform nominal doping profile but with different actual microscopic distribution of impurities, and we have computed the threshold voltage dispersion for the above mentioned devices.

1 Introduction

The continuous downscaling of MOSFET geometries, that allows higher clock frequency, lower power dissipation and increasing circuit complexity, has reached a point in which quantum confinement significantly affects device properties [1, 2]. The reduced gate oxide thickness and the increased bulk doping, required to control short-channel effects, cause a high electric field in the direction perpendicular to the Si/SiO_2 interface, strongly confining charge carriers in the channel and splitting the density of states in the channel in well-separated 2D subbands. Therefore, semiclassical models are no longer suitable to describe sub-0.1μm MOSFETs. The effect of quantum confinement on MOSFET threshold voltage has been investigated by Fiegna *et al*. [3] in a one-dimensional MOS structure. In Ref. [4] a 2D self-consistent model has been used to simulate n-MOS transistors, while in Ref. [5] the charge distribution in ultrasmall MOSFET has been computed by solving the 2D Schrödinger equation. However, to evaluate the effect of the discrete distribution of inpurities, a 3D simulation must be performed.

We have developed a code for the simulation in three dimensions of MOSFETs with ultranarrow channel, taking into account quantum confinement in the channel and depletion of the polysilicon gate. The Poisson-Schrödinger equation has been discretized with the Box-Integration method and solved using the Newton-Raphson algorithm.

We present results for the so-called "Well tempered" bulk-Si n-MOSFETs with channel length and width of 90, 50 and 25 nm proposed by D. Antoniadis [6] (the 25 nm device in basically that proposed in Ref. [7]). As we shall show, quantum confinement increases the threshold voltage by up to 170 mV for the smaller devices.

We have also considered the effects of the random distribution of dopants on the threshold voltage pf "well tempered" MOSFETs. Indeed, as the scaling down of device geometries reaches the deep submicrometer region, the number of doping atoms in the depletion region is of the order of hundreds. Consequently, intrinsic fluctuations of the number and of the position of the atoms strongly influence the value of the threshold voltage, as pointed out in several papers [8, 9, 10, 11]. Here, we will take into account at the same time the effect of random dopants, by performing a three-dimensional simulation, and the effect of quantum confinement on threshold voltage, by solving the Schrödinger equation in the channel.

2 Model

The potential profile in the three-dimensional simulation domain shown in Fig. 1 obeys the Poisson equation

$$\begin{aligned}\nabla\left[\epsilon(\vec{r})\nabla\phi(\vec{r})\right] \\ = \quad -q\left[p(\vec{r})-n(\vec{r})+N_D^+(\vec{r})-N_A^-(\vec{r})\right], \quad (1)\end{aligned}$$

where ϕ is the electrostatic potential, ϵ is the dielectric constant, p and n are the hole and electron densities, respectively, N_D^+ is the concentration of ionized donors and N_A^- is the concentration of ionized acceptors. While hole, acceptor and donor densities are computed in the whole domain with the semiclassical approximation, the electron concentration, in regions where confinement is strong, needs to be computed by solving the Schrödinger

equation with density functional theory. The observation that quantum confinement is strong only along the direction perpendicular to the Si/SiO$_2$ interface has led us to decouple the Schrödinger equation into a 1D equation in the vertical direction and a 2D equation in the $y-z$ plane: the density of states in the horizontal plane is well approximated by the semiclassical expression, since there is no in-plane confinement, while discretized states appear in the vertical direction.

The expression of the single particle Schrödinger equation in 3D, with anisotropic effective mass reads

$$-\frac{\hbar^2}{2}\frac{\partial}{\partial x}\frac{1}{m_x}\frac{\partial}{\partial x}\Psi-\frac{\hbar^2}{2}\frac{\partial}{\partial y}\frac{1}{m_y}\frac{\partial}{\partial y}\Psi \\ -\frac{\hbar^2}{2}\frac{\partial}{\partial z}\frac{1}{m_z}\frac{\partial}{\partial z}\Psi+V\phi=E\Psi \qquad (2)$$

we can write the wave function $\Psi(x,y,z)$ as

$$\Psi(x,y,z)=\psi(x,y,z)\chi(y,z) \qquad (3)$$

Substituting (3) in (2) we obtain the following expression

$$-\frac{\hbar^2}{2}\chi\frac{\partial}{\partial x}\frac{1}{m_x}\frac{\partial}{\partial x}\psi \\ -\left[\frac{\hbar^2}{2}\frac{\partial}{\partial y}\frac{1}{m_y}\frac{\partial}{\partial y}+\frac{\hbar^2}{2}\frac{\partial}{\partial z}\frac{1}{m_z}\frac{\partial}{\partial z}\right]\psi\chi \\ +V\psi\chi=E\psi\chi \qquad (4)$$

where dependence on x , y and z is implicit. If ψ satisfies the Schrödinger equation along the x direction

$$-\frac{\hbar^2}{2}\frac{\partial}{\partial x}\frac{1}{m_x}\frac{\partial}{\partial x}\psi+V\psi=E_1(y,z)\psi \qquad (5)$$

we can write

$$-\left[\frac{\hbar^2}{2}\frac{\partial}{\partial y}\frac{1}{m_y}\frac{\partial}{\partial y}+\frac{\hbar^2}{2}\frac{\partial}{\partial z}\frac{1}{m_z}\frac{\partial}{\partial z}\right]\psi\chi \\ +\left[-\frac{\hbar^2}{2}\frac{\partial}{\partial x}\frac{1}{m_x}\frac{\partial}{\partial x}\psi+V\psi\right]\chi=E\psi\chi \qquad (6)$$

and substituting (5) in (6) we obtain

$$-\left[\frac{\hbar^2}{2}\frac{\partial}{\partial y}\frac{1}{m_y}\frac{\partial}{\partial y}+\frac{\hbar^2}{2}\frac{\partial}{\partial z}\frac{1}{m_z}\frac{\partial}{\partial z}\right]\psi\chi \\ +E_1(y,z)\psi\chi=E\psi\chi \qquad (7)$$

Assuming that $\psi(x,y,z)$ is weakly dependent on y and z, equation (7) can be approximated as

$$-\left[\frac{\hbar^2}{2}\frac{\partial}{\partial y}\frac{1}{m_y}\frac{\partial}{\partial y}+\frac{\hbar^2}{2}\frac{\partial}{\partial z}\frac{1}{m_z}\frac{\partial}{\partial z}\right]\chi \\ +E_{1i}(y,z)\chi=E\chi, \qquad (8)$$

where E_{1i} is the i-th eigenvalue of (5).

Since $E_{1i}(y,z)$ in the cases considered is rather smooth in y and z, we will assume that eigenvalues of Eq. (8) essentially obey the 2D semiclassical density of states.

The confining potential V can be written as $V=E_C+V_{exc}$, where E_C is the conduction band and V_{exc} is the exchange-correlation potential within the local density approximation [12]:

$$V_{exc}=-\frac{q^2}{4\pi^2\varepsilon_0\varepsilon_r}\left[3\pi^3 n(\vec{r})\right]^{\frac{1}{3}}. \qquad (9)$$

Anisotrophy of electron effective mass in silicon must be taken into account. Solving the Schrödinger equation while considering the effective masses along the three directions in k-space, the electron density in confined regions becomes

$$n(x) = \frac{2k_BTm_t}{\pi\hbar^2}\sum_i|\psi_{li}|^2\ln[1+\exp(\frac{E_F-E_{li}}{k_BT})] \\ + \frac{4k_BT\sqrt{m_lm_t}}{\pi\hbar^2}\sum_i|\psi_{ti}|^2\ln[1+\exp(\frac{E_F-E_{ti}}{k_BT})] \qquad (10)$$

where ψ_{li}, E_{li}, ψ_{ti} and E_{ti} are the eigenfunctions and eigenvalues obtained from the one-dimensional Schrödinger equation using the longitudinal effective mass m_l and the transverse effective mass m_t, respectively.

To solve self-consistently the Poisson-Schrödinger equation, we have used the Newton-Raphson method with a predictor/corrector algorithm close to that proposed in [13]. In particular, the Schrödinger equation is not solved at each Newton-Raphson iteration step. Indeed, if we consider the eigenfunctions constant within a loop and the eigenvalues varied by a quantity of about $q(\phi-\tilde{\phi})$, where $\tilde{\phi}$ is the potential used to solve the Schrödinger equation and ϕ is the potential at the current iteration, then the electron density becomes

$$n(x) = \frac{2k_BTm_t}{\pi\hbar^2} \\ \times \sum_i|\psi_{li}|^2\ln[1+\exp(\frac{E_F-E_{li}+q(\tilde{\phi}-\phi)}{k_BT})] \\ + \frac{4k_BT\sqrt{m_lm_t}}{\pi\hbar^2} \\ \times \sum_i|\psi_{ti}|^2\ln[1+\exp(\frac{E_F-E_{ti}+q(\tilde{\phi}-\phi)}{k_BT})] \qquad (11)$$

The algorithm is then repeated cyclically until the norm of $\phi-\tilde{\phi}$ is smaller than a predetermined value.

3 Results and discussion

The considered devices have the structure depicted in Fig. 1 and the doping profiles of the "Well tempered" MOSFETs suggested by D.Antoniadis [6]. Doping profiles are shown in Fig. 2 for the 25 nm channel length device, in Fig. 3 for the 50 nm channel length device, and

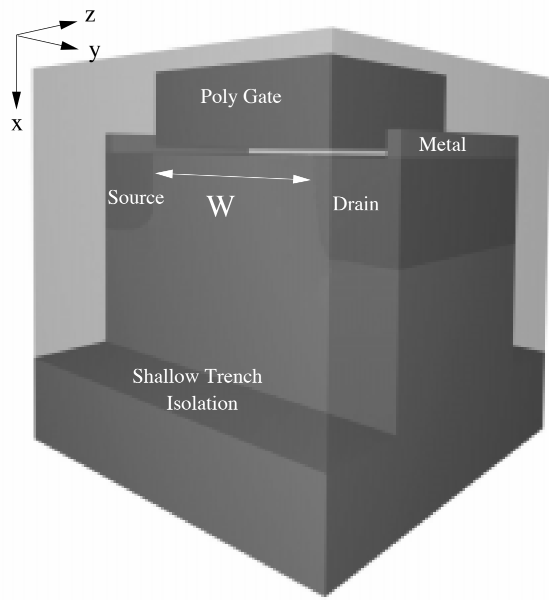

Figure 1: Three-dimensional structure of the simulated MOSFETs

in Fig. 4 for the 90 nm channel length device. Source and drain doping profiles are gaussian and very close to that actually obtained, while the super halo doping is implanted in the channel in order to reduce charge sharing effects that become important in such geometries.

The conduction band profile in the x-z plane for the 90 nm channel length device is plotted in Fig. 5, while the eigenfunctions and the eigenvalues of the Schrödinger equation in the vertical direction at the center of the channel are plotted in Fig. 6: as can be seen, the first eigenvalue, corresponding to the botton of the first subband, is more than 200 mV above the minimum of the conduction band and the peak of the first eigenfunc-

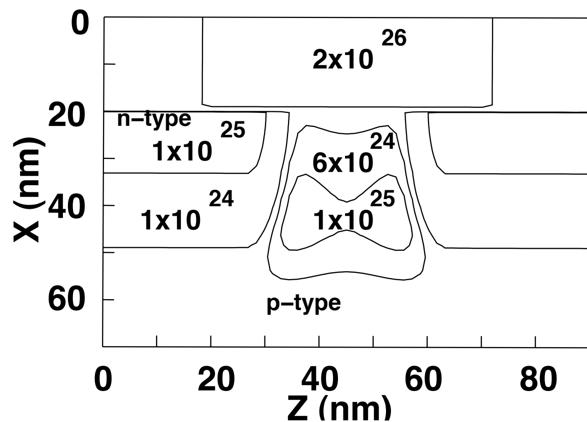

Figure 2: Difference between donor and acceptor concentrations for a MOSFET with channel length of 25 nm

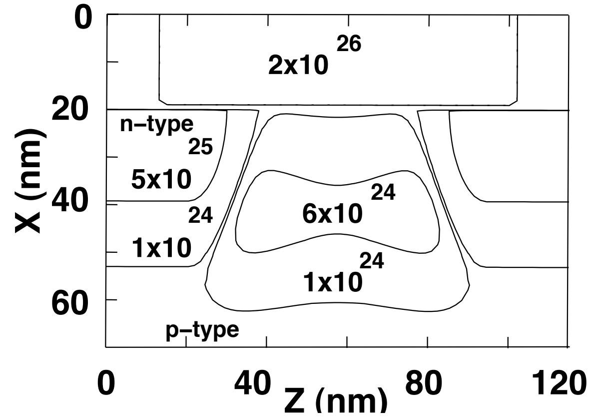

Figure 3: Difference between donor and acceptor concentrations for a MOSFET with channel length of 50 nm

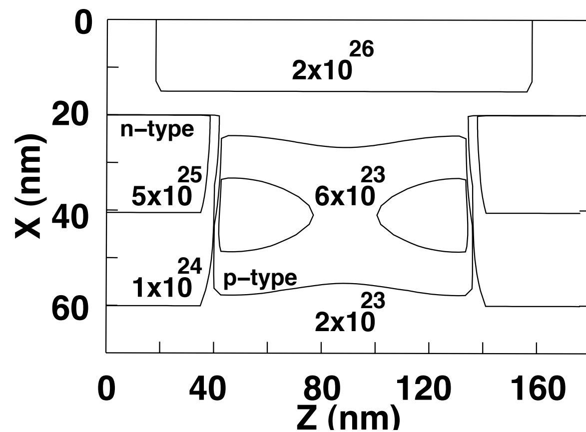

Figure 4: Difference between donor and acceptor concentrations for a MOSFET with channel length of 90 nm

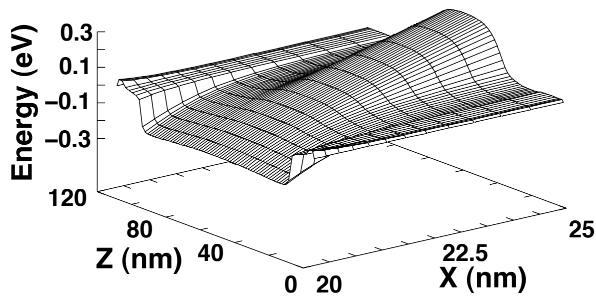

Figure 5: Conduction band of the 90 nm MOSFET in the x-z plane at inversion

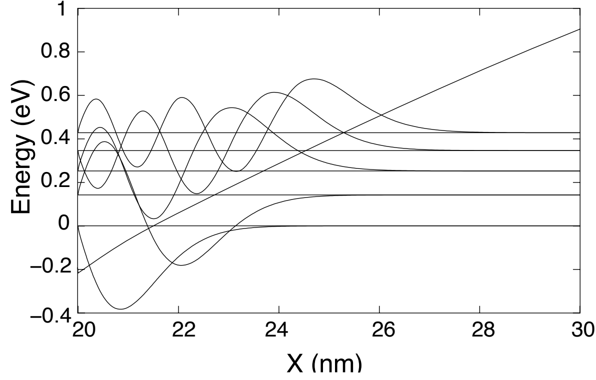

Figure 6: Conduction band profile at the center of the channel for the 90 nm MOSFET and discrete energy levels with associated eigenfunctions in the vertical direction

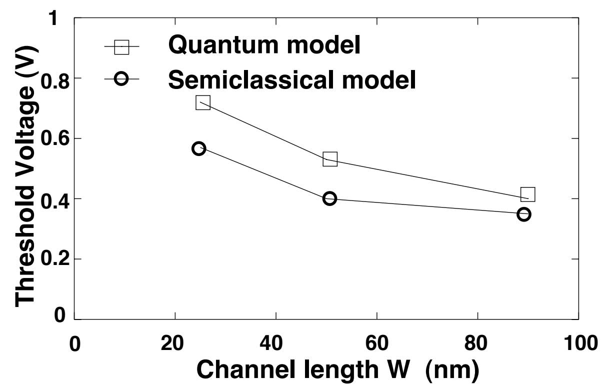

Figure 7: Threshold voltage as a function of the channel length W

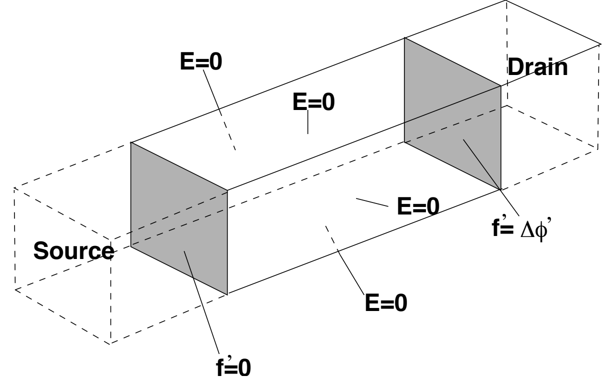

Figure 8: Boundary condition in the region belonging to the channel and used to compute the conductance

tion is about 1 nm from the Si-SiO_2 interface. As is well known, these two aspects are responsible for increased threshold voltage and degraded transconductance.

The threshold voltage increase due to quantum confinement has been evaluated quantitatively for the three MOSFET structures considered.

In Fig. 7 we plot both the threshold voltages obtained with the model described above and with a semiclassical model: the difference, as expected, increases with decreasing channel length (due to decreasing oxide thickness and increasing channel doping).

We compute V_T from the curve of channel conductance as a function of gate voltage, as the intercept of the line approximating the curve in the strong inversion region with the horizontal axis. The drain to source voltage V_{DS} is set to zero. The assumption of zero V_{DS} is a limitation of our approach and does not allow us to take into account drain-induced barrier lowering. In addition, the definition of V_T we use can give a different value compared to other commonly used definitions [1]. However, we believe that our evaluation of V_T-shift due to quantum confinement is quantitatively accurate.

For small V_{DS} and $V_{GS} > V_T$ the current has the following expression

$$I_D = \mu_n \frac{W}{L} C_{ox}(V_{GS} - V_T)V_{DS} \tag{12}$$

where μ_n is the electron mobility in the channel and C_{ox} is the oxide capacitance per unit area. For simplicity we assume constant electron mobility $\mu_n = 700\ \mathrm{cm^2V^{-1}s^{-1}}$ The conductance g_0 is therefore

$$g_0 = \frac{\partial I_D}{\partial V_{DS}} = \mu_n \frac{W}{L} C_{ox}(V_{GS} - V_T) \tag{13}$$

In the plane g_0-V_{GS}, V_T is the intercept of the curve given by (13) with the V_{GS} axis.

The conductance is computed as follows. In the drift-diffusion model the current density can be written as

$$\vec{J}_n = -qn\mu_n \nabla\phi + qD\nabla n \tag{14}$$

where D is the electron diffusion coefficient.

For each MOSFETs structure we can consider a region belonging to the channel as shown in Fig. 8. If ϕ_0 is the potential profile computed with $V_{DS} = 0$, we can write

$$0 = -qn_0\mu_n \nabla\phi_0 + qD\nabla n_0, \tag{15}$$

where n_0 is the electron density at equilibrium. By applying null Neumann boundary conditions on lateral faces and a small voltage of voltage $\Delta\phi$ between the surfaces in the proximity of the source and drain as described in Fig. 8, by considering the variation the diffusion current negligible with respect to the drift term, we have

$$\vec{J}_n = -qn_0\mu_n\nabla\phi', \tag{16}$$

where $\phi' = \phi - \phi_0$. The continuity equation

$$\nabla \cdot \vec{J}_n = 0 \tag{17}$$

gives us

$$\nabla \cdot (n_0\nabla\phi') = 0 \tag{18}$$

Solving this linear system we find ϕ' from which we can obtain $\vec{J}_n$ and therefore g_0.

3.1 Threshold voltage dispersion

As MOSFET scaling approaches the sub-100 nm regime, the number of impurity atoms is of the order of hundreds in the channel depletion region. Intrinsic dopant fluctuations determine a significant dispersion of the threshold voltage. Since, as we have seen, the threshold voltage is also significantly affected by quantum confinement in the channel, we believe both aspects have to be included in an accurate simulation. Our code allows us to solve in 3D the poisson equation, and therefore to take into account the "atomistic" distribution of impurities, and to include quantum confinement by solving the Schrödinger equation in the vertical direction. Three-dimensional semiclassical simulations of the effect of random dopants have appeared in the literature [8, 9], and quantum effects have been included with the density-gradient formalism [11].

We have assumed that the implanted ions in the channel obey the Poisson distribution. In particular, for each gridpoint we have considered the associated volume element and multiplied its volume ΔV by the nominal doping concentration. Then, a random number N' has been extracted with Poisson distribution and divided by ΔV in order to have the "actual" doping concentration in the volume element. The standard deviation of V_T has been then obtained by simulating a large number of devices with the same nominal doping, but with different actual dopant distribution. Figs. 9 , 10 and 11 show the distribution of threshold voltage computed on an ensemble of 100 nominally identical devices : V_{Tnom} is the threshold voltage in case of uniform doping distribution.

4 Conclusion

We have developed a three-dimensional Poisson/Schrödinger solver and we have simulated three nanoscale "Well tempered" MOSFETs. In the considered devices the quantum confinement is

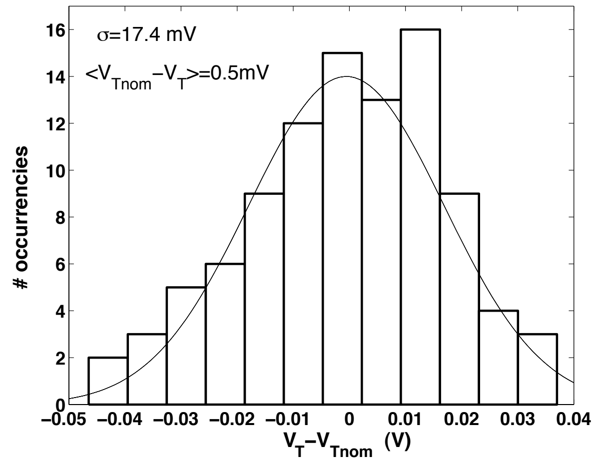

Figure 9: Threshold voltage dispersion in a 25-nm MOSFET

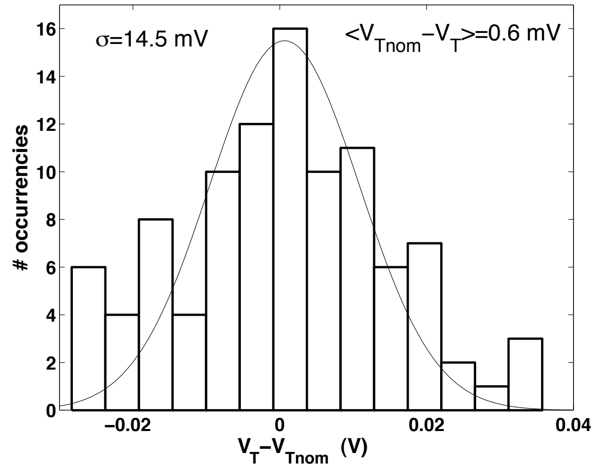

Figure 10: Threshold voltage dispersion in a 50-nm MOSFET

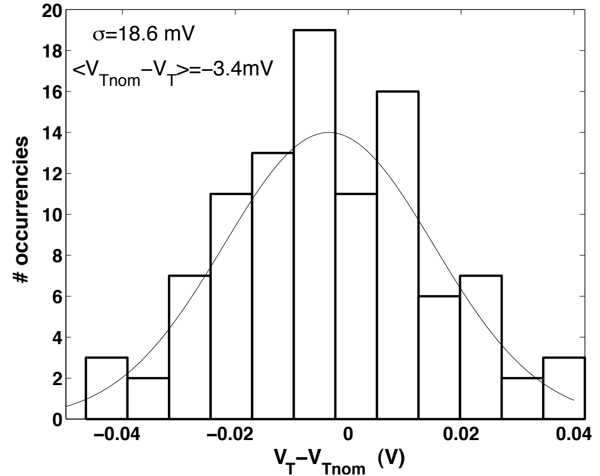

Figure 11: Threshold voltage dispersion in a 90-nm MOSFET

relevant along the x direction, so we have solved the Schrödinger equation only in one dimension, with reduced computational requirements with respect to a full 3D quantum model. Simulations have shown that the threshold voltage shift due to quantum confinement is significant and increases with device scaling down: a quantum simulation is therefore required to obtain results in quantitative agreement with experiments. As geometries scale down, also the effect of the discrete distribution of dopants becomes important and affects important properties such as the threshold voltage. Our code has allowed us to take into account simultaneously the effects of the random distribution of dopants and of quantum confinement in the channel on threshold voltage.

5 Acknowledgments

Support from the NANOTCAD Project (IST-1999-10828 NANOTCAD) is gratefully acknowledged.

References

[1] Y.Taur and T.H. Ning, *Fundamentals of Modern VLSI devices*, Cambridge University Press 1998

[2] Y. Taur, D. A. Buchanan, W. Chen, D. J. Frank, K. E. Ismail, S. H. Lo, G. A. Sail-Lalasz, R. G. Viswanathan, H. J. C. Wann, S. J. Wind, H. S. Wong, *CMOS scaling into the Nanometer Regime*, Proceedengs of the IEEE, 85(4): 486-504, 1997.

[3] C. Fiegna, A. Abramo, *Analysis of Quantum Effects in Nonuniformly Doped MOS Structures*, IEEE Trans. Electron Devices 45(4): 877-880, April 1998.

[4] A. Spinelli, A. Benvenuti, A. Pacelli, *Self-Consistent 2-D Model for Quantum Effects in n-MOS Transistors*, IEEE Trans. Electron Devices, 45(6): 1342-1349, June 1998.

[5] A. Abramo, A. Cardin, L. Selmi, E. Sangiorgi, *Two-dimensional quantum mechanical simulation of charge distribution in Silicon MOSFETs*, IEEE Trans. Electron Devices, 47(10): 1858-1863, October 2000.

[6] http://www-mtl.mit.edu/Well

[7] Y. Taur, C. H. Wann, D. J. Frank *25 nm CMOS Design Consideration*, in Proc. IEDM 1998 Tech. Dig. 789-792, 1998.

[8] H.-S. Wong, Y. Taur "Three dimensional 'atomistic' simulation of discrete random dopant distribution effects in sub-0.1 μm MOSFET's", Proc. IEDM 1993. Dig. Tech. Papers. 705-708, 1993.

[9] A. Asenov, *Random dopant induced threshold voltage lowering and fluctuations in sub 0.1 μm MOSFETs: A 3D "atomistic" simulation study"*, IEEE Trans. Electron Devices, 45: 2505, 1998.

[10] D. J. Frank, Y. Taur, M. Ieong, Hon-Sum P.Wong, *Monte Carlo Modeling of Threshold Variations due ti Dopant Fluctuations*, 1999 Symposium on VLSI Circuits Digest of Technical Papers.

[11] A. Asenov, G. Slavcheva, A. R. Brown, J. H. Davies, S. Saini, *Quantum mechanical enhancement of the random dopant induced threshold voltage fluctuations and lowering in sub 0.1 micron MOSFETs*, IEDM Tech. Digest 535-538, 1999.

[12] J. C. Inkson, *Many body theory of solids - an introduction*, Plenum, New York, 1984

[13] A. Trellakis, A.T. Galick, A. Pacelli, U. Ravaioli, *Iteration Scheme for the solution of the two-dimensional Schrödinger Poisson equations in quantum structures*, J. Appl. Phys, vol. 81(12): 7800-7804, 1997.